WASP-24b: A New Transiting Close-in Hot Jupiter orbiting a late F-star.

R.A. Street[1]

Las Cumbres Observatory Global Telescope Network, 6740 Cortona Drive, Suite 102, Goleta, CA 93117, U.S.A.

and

E. Simpson[2], S.C.C. Barros, D. Pollacco, Y. Joshi

Astrophysics Research Centre, Physics Building, Queen's University, Belfast, County Antrim, BT7 1NN, United Kingdom.

and

A.Collier Cameron[3], R. Enoch, N. Parley

SUPA, School of Physics and Astronomy, University of St. Andrews, North Haugh, St. Andrews, KY16 9SS, United Kingdom.

and

E. Stempels[4]

Department of Physics and Astronomy, Box 516, SE-751 20 Uppsala, Sweden

and

L. Hebb[5]

Physics & Astronomy Department, Vanderbilt University, 1807 Station B, Nashville, TN 37235, U.S.A.

and

A.H.M.J. Triaud, D. Queloz, D. Segransan, F. Pepe, S. Udry[6]

Observatoire Astronomique de l'Université de Genève, 51 Chemin des Maillettes, 1290 Sauverny, Switzerland.

and

T.A. Lister, É. Depagne[1]

Las Cumbres Observatory Global Telescope Network, 6740 Cortona Drive, Suite 102, Goleta, CA 93117, U.S.A.

and

R.G. West[7]

Department of Physics & Astronomy, University of Leicester, University Road, Leicester, LE1 7RH, United Kingdom

and

A.J. Norton[8]

N2041, Venables Building, Dept. of Physics & Astronomy, The Open University, Milton Keynes, MK7 6AA, United Kingdom

and

B. Smalley[9], C. Hellier, D.R. Anderson, P.F.L. Maxted, S.J. Bentley

Astrophysics Group, Keele University, Staffordshire, ST5 5BG, United Kingdom

and

I. Skillen[10]

Isaac Newton Group of Telescopes, Apartado de correos 321, E-38700 Santa Cruz de la Palma, Canary Islands, Spain

and

M. Gillon[11]

Institut d'Astrophysique et de Géophysique, Université de Liège, Allée du 6 Août 17, Bat. B5C, 4000 Liège, Belgium

Received _____; accepted _____

ABSTRACT

We report the discovery of a new transiting close-in giant planet, WASP-24 b, in a 2.341 d orbit, 0.036 AU from its F8-9 type host star. By matching the star's spectrum with theoretical models, we infer an effective temperature $T_{\rm eff}$=6075±100 K and a surface gravity of $\log g$=4.15±0.10. A comparison of these parameters with theoretical isochrones and evolutionary mass tracks places only weak constraints on the age of the host star, which we estimate to be $1.6^{+2.1}_{-1.6}$ Gyr. The planetary nature of the companion was confirmed by radial velocity measurements and additional photometric observations. These data were fit simultaneously in order to determine the most probable parameter set for the system, from which we infer a planetary mass of $1.032^{+0.038}_{-0.037}\,M_{\rm Jup}$ and radius $1.104^{+0.052}_{-0.057}\,R_{\rm Jup}$.

Subject headings: stars: planetary systems: individual: WASP-24b, techniques: photometric, techniques: spectrographs

1. Introduction

Large scale, ground-based surveys for transiting planets are yielding a surprisingly diverse set of close-in giant planets. The last few years have seen the discovery of a number of so-called 'bloated' close-in Jovian planets, for example WASP-17 b (Anderson et al. 2010) and Kepler-7 b (Latham et al. 2010). The very low densities of these objects present an ongoing challenge to theories of planet formation and evolution (Fortney et al. (2008), Guillot et al. (2006), Burrows et al. (2007)). Ultra-short period planets such as WASP-19 b (Hebb et al. 2010) offer a testbed for the physics of the dissipation of tidal energy, thought to both bolster the planetary radius (Fortney et al. (2007), Burrows et al. (2007)) and perhaps cause the planet's orbits to decay (Jackson et al. 2009), ultimately leading to them spiraling into their host stars. Each new wave of planets discovered has produced new surprises. As the surveys searching for new systems reach maturity, and are complemented by targeted space-based missions, we are populating a wider range of the planetary orbital and physical parameter space. A more complete picture of the planetary menagerie will lead to a better understanding of the formation and evolutionary forces at work.

There is particular value in completing a census of the transiting planets of bright stars, which is evident from the extraordinary insights offered by follow-up work into the composition, structure and even weather of their atmospheres and exospheres (e.g. Désert et al. (2009), Knutson et al. (2009), Burrows et al. (2009) & references therein). We may even be able to detect changes in weather patterns over the course of an orbit for the long period and eccentric planets (Iro & Deming 2010). Ground-based instruments survey large numbers of bright stars spanning spectral types F–M and produce targets well suited for further study.

We report the discovery of a new close-in giant planet orbiting an 11.3 mag, F8-9 type host star. Our observations are described in Section 2, including both our discovery data

and follow-up work. In Section 3 we present the fitting procedure from which we determine the overall system parameters. We discuss the new system in the context of the current sample of known planets in Section 4.

2. Observations

2.1. SuperWASP Discovery Data

The WASP Consortium[1] operates two fully robotic, dedicated observatories: WASP-North, sited at the Observatorio del Roque de los Muchachos (ORM), La Palma, Canary Islands, Spain and WASP-South, hosted by the South African Astronomical Observatory at Sutherland, South Africa. Both stations support 8 cameras, each consisting of a Canon 200 mm, f/1.8 lens and an Andor 2048×2048 pixel thinned e2v CCD. Each camera has a 7.8×7.8 degree field of view and a pixel scale of 13.7″/pixel. Every clear night the stations execute pre-set observing programs, repeatedly imaging a sequence of 6–12 planet fields every ∼8 mins for as long as they are visible. Full details of the hardware and data reduction procedures are given in Pollacco et al. (2006). Cameron et al. (2006) describes the HUNTSMAN algorithm used to search the data for transits.

WASP-North and -South have been observing WASP-24 since 2008 March 5, accumulating a lightcurve of 9750 datapoints by 2009 April 28, shown in Figure 1. Once flagged by HUNTSMAN, the WASP lightcurve for this star was manually evaluated along with all available catalog data (for a description of our selection procedure, see Cameron et al. (2007)), and the object was put forward for follow-up.

[1]www.superwasp.org

2.2. Spectroscopic Follow-Up

The 2.56m Nordic Optical Telescope, sited at ORM, La Palma, provided the first radial velocity measurements of the WASP-24 system. The Fibre-Fed Echelle Spectrograph (FIES) was used in medium resolution mode (R = 46,000) with simultaneous ThAr wavelength calibration, giving spectra covering the wavelength range 370–720 nm. A total of 10 spectroscopic observations were made between 2008 December 31 and 2009 April 10 with an exposure time of 1200s. The data were reduced using the bespoke package FIEStool and an IDL cross-correlation routine was used to derive the radial velocities.

Additional radial velocity measurements were obtained between 2009 Jan 29 and 2009 July 26 with the CORALIE Fibre-Fed Echelle Spectrograph on the Swiss 1.2-m Leonard Euler telescope at ESO-La Silla, Chile. These spectra span the wavelength range 390–690 nm with a resolution ∼50,000. The radial velocity measurements derived from both datasets are given in Table 1, and plotted in Figure 2.

These spectra showed no sign of the broadened lines which would indicate a rapidly rotating host star and make any planetary companion difficult to confirm. Nor did it exhibit the dual lines of a spectroscopic binary. The amplitude of variation was only $0.1451^{+0.0046}_{-0.0046}\,\mathrm{km\,s^{-1}}$, indicating a companion of planetary mass. To exclude the possibility that this signal was caused by stellar activity, span bisector analysis was performed (Queloz et al. 2001). Figure 2 (lower panel) shows that no significant variation was seen. In addition, these data would be expected to display a gradient if the RV signal were caused by a massive companion such as a brown dwarf orbiting an unresolved binary (Santos et al. 2002). As no slope was seen we concluded that the signal is due to an orbiting planetary companion. The star was therefore promoted in the target list for higher resolution imaging and photometry.

Table 1: Radial velocity observations of WASP-24.

NOT data			CORALIE data		
HJD-2450000	RV (km/s)	RVerror(km/s)	BJD-2450000	RV (km/s)	RVerror(km/s)
4832.7716	-17.745	0.012	4860.880663	-17.652	0.022
4833.8017	-18.054	0.014	4894.849549	-17.916	0.022
4834.7794	-17.735	0.015	4895.848219	-17.647	0.015
4835.7779	-17.989	0.028	4896.864309	-17.937	0.018
4836.7888	-17.902	0.018	4897.806121	-17.731	0.016
4862.7251	-17.778	0.022	4898.855187	-17.841	0.018
4910.6468	-18.008	0.012	4941.751321	-17.912	0.015
4922.6956	-18.105	0.018	4942.798648	-17.691	0.018
4931.6231	-17.877	0.030	4943.776517	-17.952	0.018
4932.5743	-17.967	0.019	4944.765090	-17.701	0.017
			4946.758076	-17.815	0.015
			4947.721482	-17.729	0.015
			4948.696148	-17.961	0.014
			4950.799019	-17.915	0.017
			4972.742729	-17.718	0.018
			4985.671129	-17.891	0.015
			5013.591181	-17.803	0.020
			5038.504437	-17.675	0.017

2.3. Photometric Follow-Up

In order to better constrain the morphology of the lightcurve, we obtained photometry of additional transit events with LCOGT facilities, shown in Figure 3. With a declination of $\sim+2°$, WASP-24 is visible to both 2.0m Faulkes Telescopes. Faulkes-North (FTN, Hawai'i) observed a near-complete transit on 2009 May 17 with the Merope camera plus the SDSS-i′ filter, and a partial event on 2009 June 12. FTN and its southern counterpart Faulkes-South (FTS, Siding Spring, Australia) jointly observed the transit on 2009 July 17 using the Pan-STARRS-z filter. The Merope instruments were used at both telescopes for these events, and have similar properties. They contain an e2V 2048×2048 pixel-CCD and have a field of view of $4.7′\times4.7′$. FTN observed this star again on 2010 February 22. Only egress could be observed during this event, as the target rose during mid-transit. In this case, the Spectral camera was used with the Pan-STARRS-z filter because it offers a larger ($10.3\times10.2′$) field of view and hence more comparison stars.

2.4. Neighboring Eclipsing Binary

In the course of obtaining photometric follow-up of WASP-24, we noticed that the nearest neighboring star (hereafter called N1, see Figure 4) showed deep (∼0.8 mag), 'V'-shaped eclipses in a few, but not all, of our datasets (shown in Figure 5). This object, at α=15 08 50.3, δ=+02 20 31.8, has V=17.970 mag (NOMAD Catalog) and is identified as USNO-B1.0 0923-0348082. It is present in the 2MASS Point Source Catalog as 2MASS 15085031+0220313 with magnitudes J=14.160 mag, H=13.551 mag and K_S=13.349 mag. Although these are the combined magnitudes of two stars, the colors imply a late K/early M spectral type.

This neighboring star lies ∼21.2 arcsec from WASP-24. Although the two objects are

blended in the SuperWASP imaging, N1 is ∼6.7 mag fainter in V. N1 will have had minimal effect on the WASP transit photometry because even at its brightest it is below the limit of detectability in the SW exposures.

N1 is clearly separated from WASP-24 in the follow-up photometry, as shown by Figure 4, and was explicitly excluded from the list of comparison stars used to derive the differential photometry for the latter object. Eclipses of N1 were observed from both FTN and FTS, and the measured times of minima (Table 2) do not co-incide with the transits of WASP-24. Additionally, they show a markedly different profile and amplitude. Finally, the neighbor is sufficiently separated from WASP-24 as to fall outside the spectrograph fibre during the CORALIE and NOT observations. From this we conclude that the transits of WASP-24 are observed independently of the variability of its neighbor.

We used the Starlink package FROG (Allan 2004) to identify the period of this binary from the combined photometric datasets. This suggested a period of P=1.156 d but as the datasets do not cover the entire phase range, we cannot rule out integer multiples of this. We note that $2P$ = 2.312 d, similar to the period of WASP-24 (P=2.341 d), but sufficiently different that our photometry from 2009 May-June, timed to observed transits of WASP-24, produced out of eclipse data for N1. The ephemerides of the two objects only produced minima on the same night in data from 2009 July.

Given the depth and profile of the eclipses of N1 and its very red overall color, it is

Table 2: Times of eclipses of the neighboring EB, given in (HJD-2450000.0).

Measured T_0	Date (UT)	Telescope
5022.8319±0.0003	2009/07/10	FTN
5023.9869±0.0002	2009/07/11	FTS
5029.76805±0.00005	2009/07/17	FTN

likely to be a detached eclipsing binary of two late-type components.

3. Deriving System Parameters for WASP-24

3.1. Spectral Type

We used the high-resolution NOT spectra to derive refined estimates for the stellar atmospheric parameters $T_{\rm eff}$, surface gravity $\log g$, metallicity [M/H], projected radial velocity $v \sin i$ and Lithium abundance $\log n$(Li). The NOT spectra were analyzed using the *Spectroscopy Made Easy* package (hereafter SME; Valenti & Piskunov (1996)) to fit a sequence of synthetic spectra. The best-fitting synthetic spectrum from this grid of models was then identified via a minimum least-squares technique. Figure 6 overlays the NOT spectrum with the best-fitting synthetic model. For more details of this method, see Stempels et al. (2007). This analysis produced the estimates for the stellar atmospheric parameters given in Table 3.

The surface gravity, $\log g$=4.15±0.1, suggested that the star may have evolved away from the main sequence. This conclusion was supported by the low level of Lithium (Sestito & Randich 2005) apparent from the weak Li I (λ=678 nm) line, which implied an age of at least 1 Gyr.

3.2. Planetary System Parameters

We used an updated version of the Markov-chain Monte Carlo (MCMC) fitting procedure described by Cameron et al. (2006) and Pollacco et al. (2008) to determine the full set of system parameters by simultaneously fitting the transit photometry and radial-velocity curves. Limb-darkening parameters appropriate to the filter of each of the

Table 3: Basic parameters of the host star, including the age and mass as derived in Section 3.3. J, H, K_s magnitudes are derived from the 2MASS catalog (Cutri et al. 2003). The quoted spectral type is derived from Gray (1992) based on the effective temperature.

Identifiers	1SWASP J150851.72+022036.1
	USNO-B1.0 0923-0348089
	2MASS J15085174+0220358
	TYCHO-2 339-329-1
RA (J2000.0)	$15^h\ 08^m\ 51.72^s$
Dec (J2000.0)	$+02^\circ\ 20'\ 36.1''$
$V_{\rm SW}$	11.306 ± 0.108 mag
J	10.457 ± 0.022 mag
H	10.219 ± 0.026 mag
K_s	10.148 ± 0.023 mag
$V_{\rm SW} - K_s$	1.079 mag
$J - H$	0.238 mag
Spectral Type	F8-9
$T_{\rm eff}$	6075 ± 100 K
$\log g$	4.15 ± 0.10
[M/H]	$+0.07 \pm 0.10$
$v \sin i$	6.96 kms^{-1} inc. 4.4 kms^{-1} of macroturbulence
$\log n$(Li)	2.42 ± 0.1
Age	$1.6^{+2.1}_{-1.6}$ Gyr
Mass	$1.15^{+0.06}_{-0.05}\ M_\odot$

separate photometric datasets were included, based on the tables of Claret et al. (2000) and Claret et al. (2004).

The current version of the MCMC code computes the stellar mass as a function of $T_{\rm eff}$, $\log \rho_*$ and [Fe/H] using the procedure described by Enoch et al. (2010), based on the compilation of eclipsing-binary data by Torres et al. (2010). The code uses $T_{\rm eff}$ and [Fe/H] as MCMC jump variables, constrained by Bayesian priors based on the spectroscopically-determined values given in Table 3.

At each step, the stellar density was computed from the parameters describing the transit geometry. The stellar mass was then computed using the empirical calibration and the posterior probability distribution for the stellar mass is given in Table 4. Radial velocity observations are known to produce a bias towards small but non-zero eccentricities (Lucy & Sweeney 1971) unless the photometric data offer well-defined ingress and egress. The current data do not offer adequate constraint, so any measured eccentricity should be considered to be an upper limit. To explore this, we performed multiple runs of the fitting procedure, alternately fixing the eccentricity to zero and allowing it to float, as well as with and without a requirement that the star be on the main sequence. The star and planetary mass and radii were consistent within the formal errors for all four fits. We therefore present in Table 4 the system parameters for the e=0 case, with the star constrained to the main sequence. The appropriate model RV and lightcurves are superimposed on the datasets shown in Figures 1, 2 & 3.

3.3. Stellar Age

In order to constrain the age of this star, we used the theoretical isochrones of Girardi et al. (2000), for the measured metallicity of WASP-24, $Z = Z_{\odot}10^{[M/H]}$=0.0223, following

Table 4: System parameters for WASP-24.

Parameter	Symbol	Value	Unit
Transit epoch	T_0	$2455062.64955^{+0.00037}_{-0.00037}$	
Orbital period	P	$2.3412083^{+0.0000049}_{-0.0000045}$	days
Ratio planet/star area	$(R_p/R_s)^2$	$0.00978^{+0.00023}_{-0.00024}$	
Transit width	δt	$0.108^{+0.0012}_{-0.0012}$	days
Impact parameter	b	$0.504^{+0.05}_{-0.067}$	R_*
Stellar reflex velocity	K	$0.1451^{+0.0046}_{-0.0046}$	km/sec
Center-of-mass velocity	γ	$-17.8992^{+0.0011}_{-0.0011}$	km/sec
Orbital eccentricity	e	$0.0^{+0.0}_{-0.0}$	
Argument of periastron	ω	$0.0^{+0.0}_{-0.0}$	deg
Orbital inclination	i	$85.71^{+0.71}_{-0.59}$	deg
Stellar density	ρ_*	$0.747^{+0.096}_{-0.073}$	$\rho_\odot$
Stellar mass	M_*	$1.129^{+0.027}_{-0.025}$	$M_\odot$
Stellar radius	R_*	$1.147^{+0.044}_{-0.048}$	$R_\odot$
Orbital separation	a	$0.03593^{+0.00029}_{-0.00027}$	AU
Planet radius	R_P	$1.104^{+0.052}_{-0.057}$	$R_{\rm Jup}$
Planet mass	M_P	$1.032^{+0.038}_{-0.037}$	$M_{\rm Jup}$
Stellar surface gravity	$\log g_*$	$4.371^{+0.033}_{-0.029}$	
Planet surface gravity	$\log g_P$	$3.288^{+0.044}_{-0.038}$	
Planet density	ρ_P	$0.768^{+0.126}_{-0.096}$	$\rho_{\rm Jup}$
$L_{total}/L_{critical}$	L_{tot}/L_c	$0.5133^{+0.011}_{-0.0098}$	
Planet equil. temp. (A=0)	T_P	$1660.0^{+44.0}_{-42.0}$	K

the method of Hebb et al. (2008). We computed the value $R_*/(M_*^{1/3})$ as a proxy for stellar density, and plotted it against $T_{\rm eff}$ for isochrones in the range $\log age$=6.6 – 10.15. Similarly, we extracted evolutionary mass tracks, plotting $R_*/(M_*^{1/3})$ vs. $T_{\rm eff}$ for stars of the same mass at each epoch in the age range above.

The location of WASP-24 relative to these tracks could then be found from the star's spectroscopic $T_{\rm eff}$ and the mean stellar density, ρ_*=$0.747^{+0.096}_{-0.073}\,\rho_\odot$, derived from the MCMC fit. Taking the two isochrones and mass tracks to either side of the star's position (Figure 7), we then interpolated along all four to provide a smoothly sampled, denser grid, then found the values of stellar mass and age from the isochrone and mass track closest to the target's $R_*/(M_*^{1/3})$ and $T_{\rm eff}$. The process was repeated for the extremes of the $T_{\rm eff}$ and ρ_* error ranges to provide estimates of the uncertainties in the stellar mass and age.

From this analysis, we estimate the age of WASP-24 to be $1.6^{+2.1}_{-1.6}$ Gyr and the mass to be $1.15^{+0.06}_{-0.05}\,M_\odot$, consistent with the result of the MCMC fitting, as expected. These and other basic parameters of this host star are summarized in Table 3.

4. Discussion

Our best fit to the combined RV and photometry data indicate that WASP-24 hosts a $1.032\,M_{\rm Jup}$ planet in a circular orbit with a semi-major axis, a, of 0.03593 AU. With a radius of $1.104\,R_{\rm Jup}$, WASP-24 b lies close to the main clump of objects on the planetary mass-radius diagram. We compared the measured radius, to the theoretical predictions in Fortney et al. (2007). Their paper offers predicted radii for planets of various masses, core size, orbital separation and age. Depending on the core mass fraction, Fortney et al. (2007) predicts a radius 0.93–$1.16\,R_{\rm Jup}$ for a $1.0\,M_{\rm Jup}$ planet, which is consistent with our derived parameters.

WASP-24 b may be compared with the well-studied transiting planet HD 189733 b, with a similar orbital period, mass and radius, though with a more massive host star. As a result, the equilibrium temperature of WASP-24 b, 1659K, is higher even than HD 189733 b's dayside (1212 K, Knutson et al. (2007)). HAT-P-5 b, which is close to WASP 24 b in mass (M_P=1.06 $M_{\rm Jup}$) suffers comparable irradiation from its ∼F8 host star (P=2.79 d), but retains a slightly larger radius, at 1.26 $R_{\rm Jup}$. The systems are also similar in age (Age$_{HAT-P-5}$ = 2.6 Gyrs), but not stellar metallicity ($\left[\frac{Fe}{H}\right]_{HAT-P-5}$=0.24).

5. Acknowledgments

Based on observations made with the Nordic Optical Telescope, operated on the island of La Palma jointly by Denmark, Finland, Iceland, Norway, and Sweden, in the Spanish Observatorio del Roque de los Muchachos of the Instituto de Astrofísica de Canarias. This work made use of the Exoplanet Encyclopedia, exoplanet.eu.

Facilities: WASP, 2MASS, ViZieR, NOT, LT, FTN, FTS, Euler 1.2m, LCOGT, exoplanet.eu

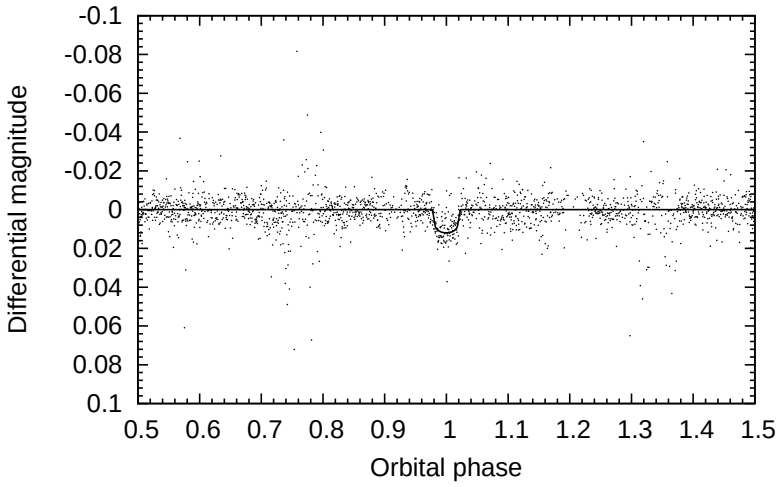

Fig. 1.— The combined WASP-North and -South lightcurve for WASP-24, folded on the ephemeris derived from this and follow-up datasets and averaged in bins of width 120 s. Superimposed is the model transit lightcurve, based on the determined system parameters.

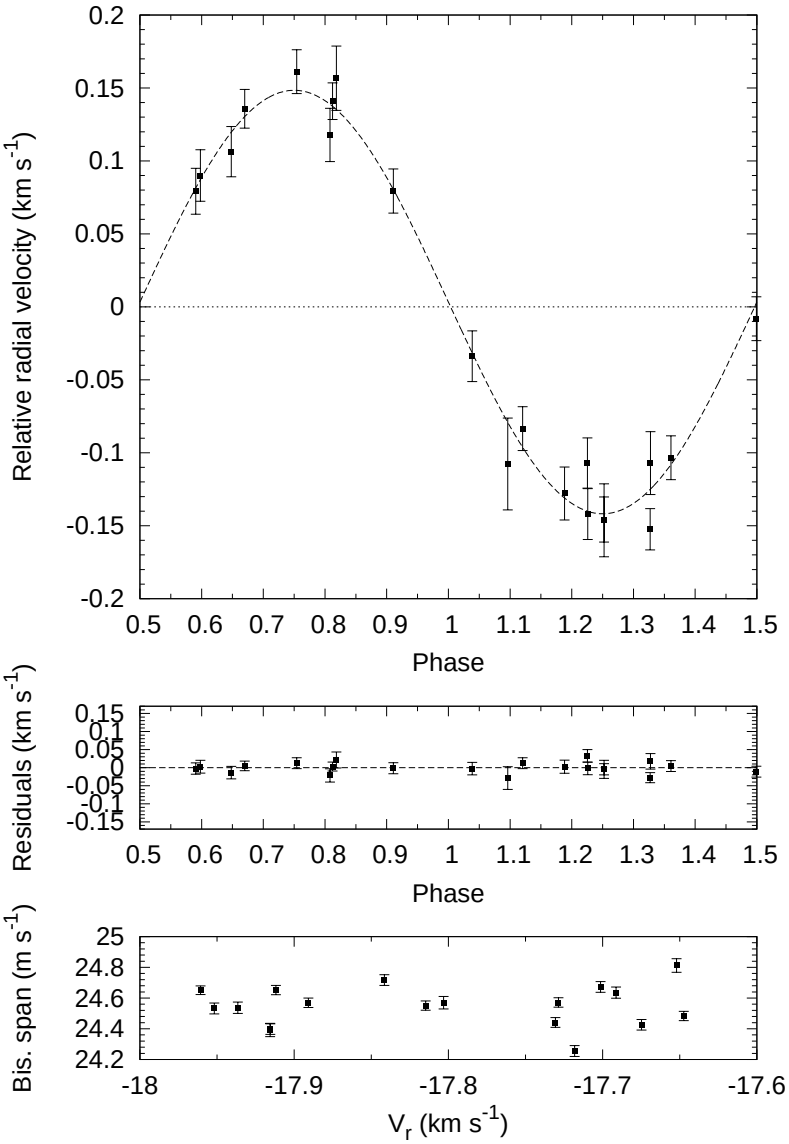

Fig. 2.— (Upper panel) Phase-folded radial velocity measurements of WASP-24, combining data from the Swiss 1.2m/CORALIE and the 2.56m NOT/FIES. (Middle panel) The RV residuals once the model for the orbital motion of the planet has been subtracted. (Lower panel) The bisector span are plotted against their measured RV.

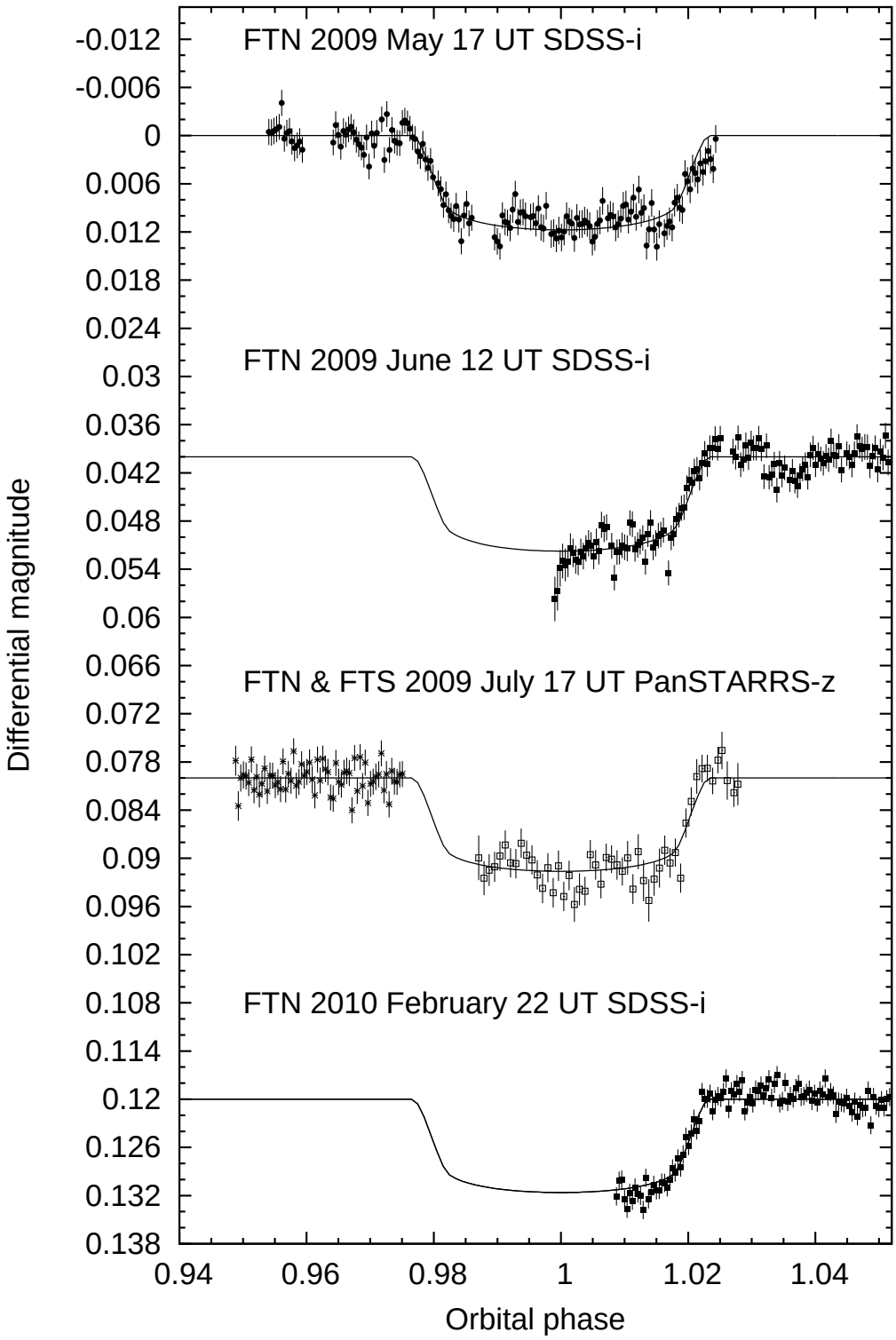

Fig. 3.— Photometry of transit events between 2009 May and 2010 February, offset in magnitude for clarity. The FTS data from 2009 July 17 (open squares) has been binned to 100s. Superimposed are the model transit lightcurves based on the determined system parameters.

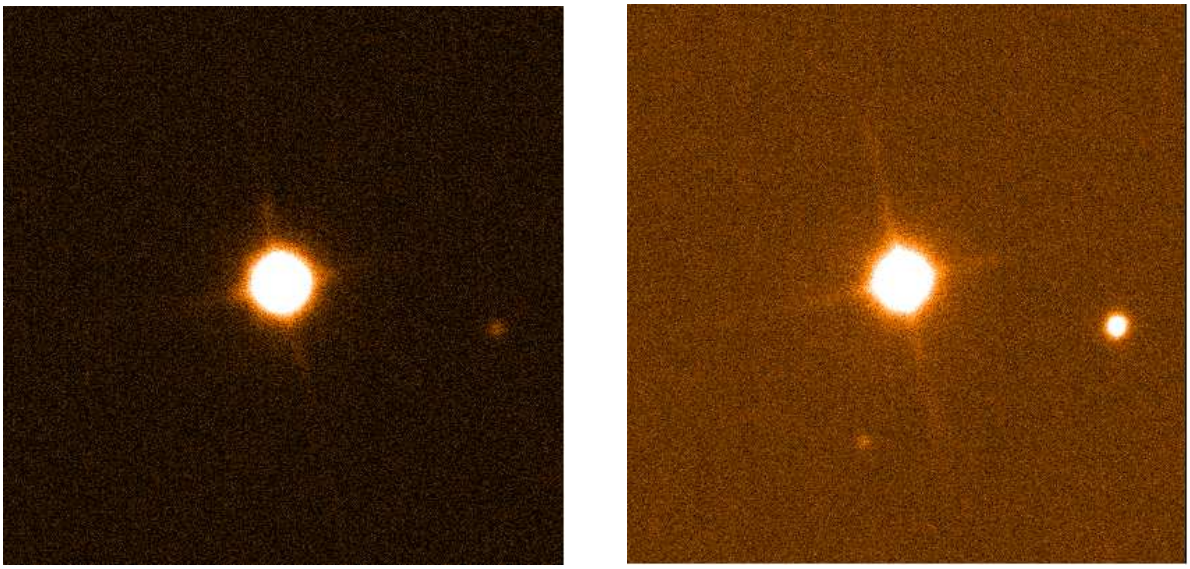

Fig. 4.— $1' \times 1'$ subframes from high resolution (pixel scale=0.139″/pixel) FTN imaging of WASP-24 in Bessel-B (left) and Pan-STARRS-z (right) passbands. North is up and East is left. The neighboring eclipsing binary is to the right of WASP-24 (center).

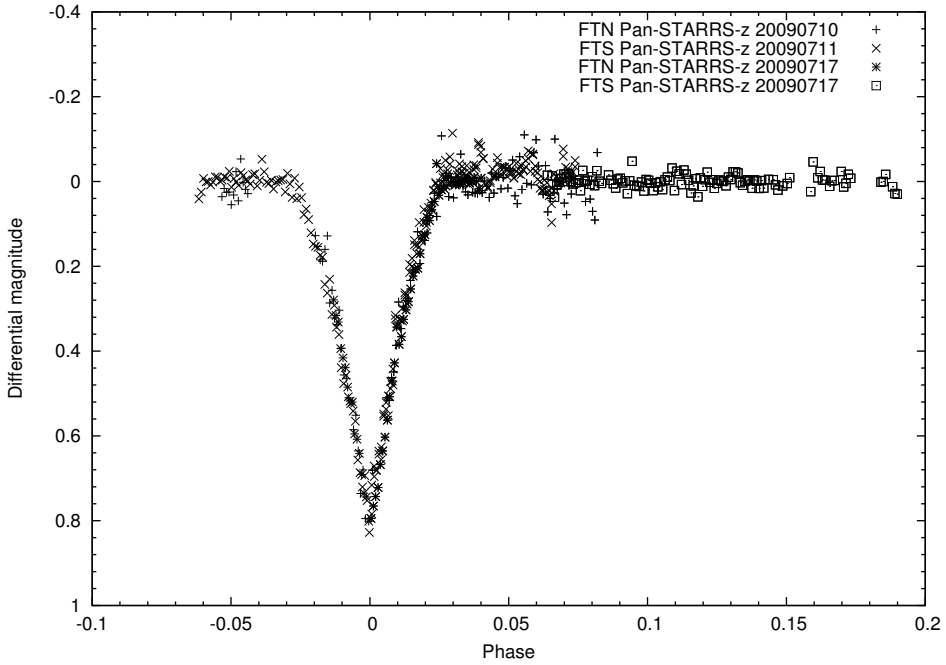

Fig. 5.— The lightcurve of the neighboring binary, folded on a period of 1.156 d and combining data from FTN and FTS in Pan-STARRS-z filter covering 3 eclipses. Other datasets in SDSS-i′ and Bessell-I were obtained out of eclipse and were combined with the Pan-STARRS-z data to constrain the period.

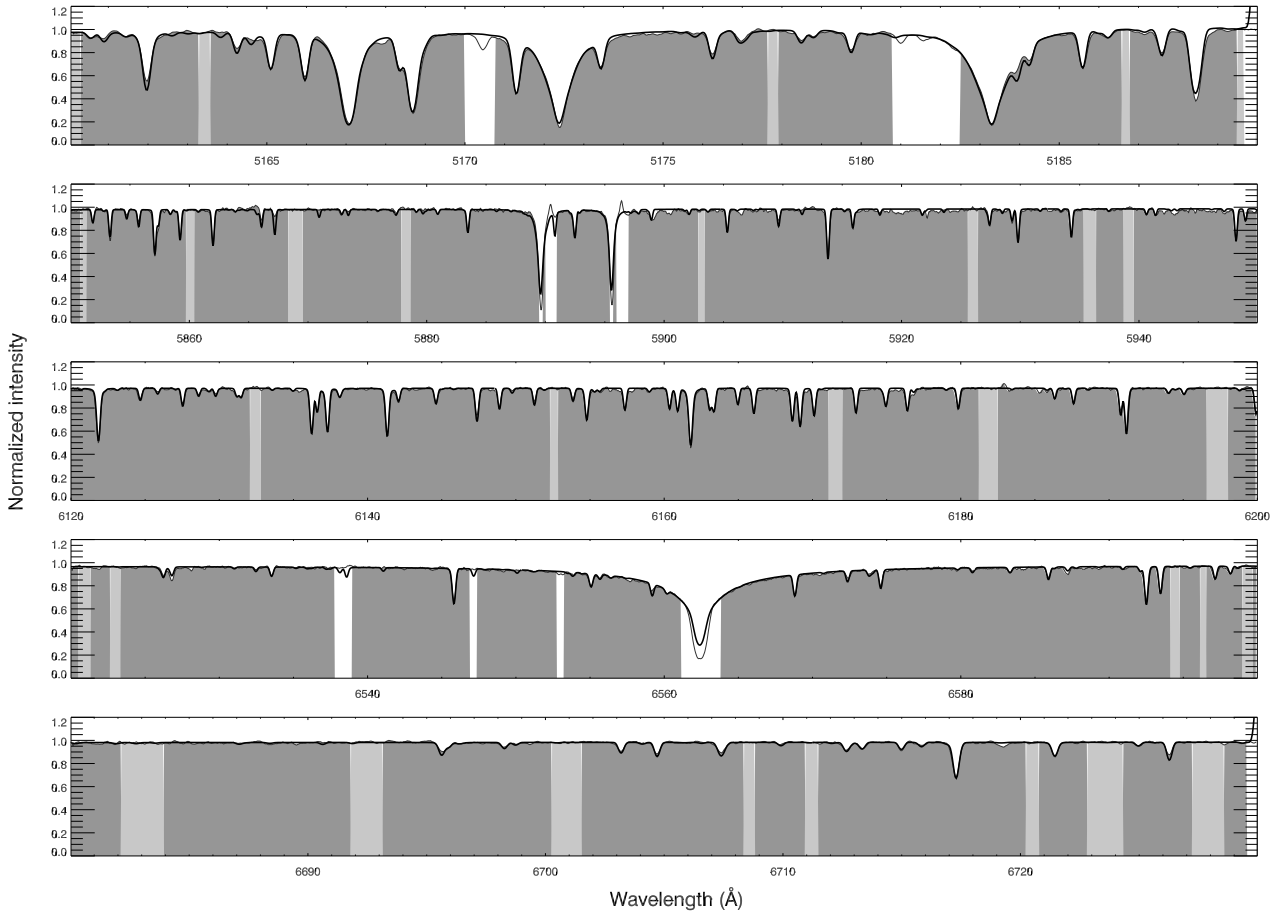

Fig. 6.— NOT spectrum overlaid with a synthetic spectrum fit during analysis with SME.

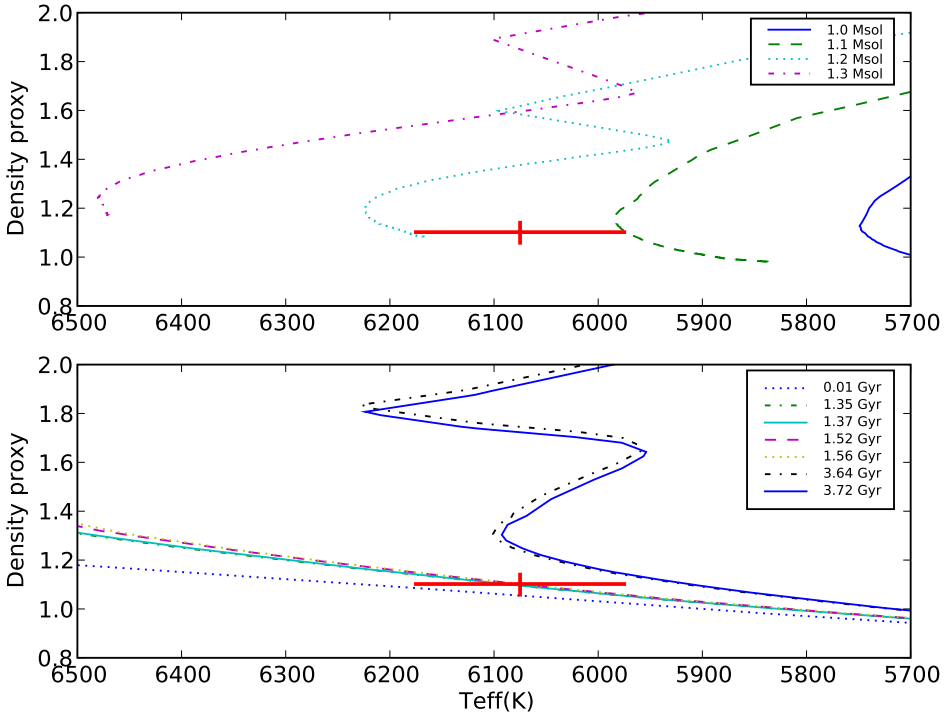

Fig. 7.— (Upper panel) Evolutionary mass tracks plotted as density proxy $R_*/(M_*^{1/3})$ against effective temperature. (Lower panel) Isochrones plotted as functions of the same parameters. Both datasets are derived from the theoretical work of Girardi et al. (2000). The position of WASP-24 is indicated with its error ranges.

REFERENCES

Agol, E. et al., 2005, MNRAS, 359, p.567.

Allan, A., 2004, Astronomical Data Analysis Software and Systems XIV, ASP Conf. Series, eds. P. Shopbell, M. Britton, R. Ebert, 347, p.370.

Anderson, D. et al., 2010, ApJ, 709, p.159.

Bean, J.L., 2009, A&A, 506, p.369.

Burrows, A. et al., 2007, ApJ, 661, p.502.

Burrows, A. & Orton, G., 2009, arXiv0910.0248.

Collier Cameron, A. et al., 2006, MNRAS,373, p.799.

Collier Cameron, A. et al., 2007, MNRAS, 380, p.1230.

Chabrier, G. & Baraffe, I., 2007, ApJ, 661, p.L81.

Claret, A., 2000, A&A, 363, p.1081.

Claret, A., 2004, A&A, 428, p.1001.

Csizmadia, S. et al., 2009, arXiv:0911.3585.

Cutri, R. M. et al., 2003, 2MASS All-Sky Catalog of Point Sources, NASA/IPAC Infrared Science Archive.

Désert, J.-M. et al., 2009, ApJ, 699, p.478.

Enoch et al.,2010, A&A, submitted.

Fortney, J.J., Marley, M.S. & Barnes, J.W., 2007, ApJ, 659, p.1661.

Fortney, J.J. et al., 2008, ApJ, 678, p.1419.

Gibson, N.P. et al., 2009, arXiv:0905.4680.

Girardi, L., 2002, A&A, 391, p.195.

Gray, D.F., 1992, The observation and analysis of stellar photospheres, 2nd ed., CUP.

Guillot, T. & Showman, A.P., 2002, A&A, 385, p.156.

Guillot, T. et al, 2006, A&A, 453, L21.

Hebb, L. et al., 2008, ApJ, 693, p.1920.

Hebb, L. et al., 2010, ApJ, 708, p.224.

Ibgui, L., Burrows, A. & Spiegel, D.S., 2009, arXiv:0910.4394.

Iro, N. & Deming, L.D., 2010, arXiv:1001.1171.

Jackson, B., Greenberg, R. & Barnes, R., 2008, ApJ, 681, p.1631.

Jackson, B. et al., 2009, ApJ, 698, p.1357.

Kipping, D.M., 2009, MNRAS, 392, p.181.

Knutson, H. et al., 2007, Nature, 447, p.183.

Knutson, H. et al., 2009, ApJ, 691, p.866.

Latham, D. et al., 2010, ApJ, submitted, arXiv.1001.0190.

Levrard, B., Winisdoerffer, C. & Chabrier, G., 2009, ApJ, 692, L9.

Lucy, L.B. & Sweeney, M.A., 1971, AJ, 76, p.544.

Miller, N., Fortney, J.J. & Jackson, B., 2009, ApJ, 702, p.1413.

Pollacco, D. et al., 2006, PASP, 118, p.1407.

Pollacco, D. et al., 2008, MNRAS, 385, p.1576.

Queloz, D. et al., 2001, A&A, 379, p.279.

Rabus, M. et al., 2009, A&A, 508, p.1011.

Santos, N.C. et al., 2002, A&A, 392, p.215.

Sestito, P.& Randich, S.,2005,A&A,442, p.615.

Steele, I.A. et al., 2008, S.P.I.E., 7014, p.70146J.

Stempels, E. et al., 2007, MNRAS, 379, p.773.

Torres, G., Andersen, J.& Gimnez, A., 2010, A&A Rev., 18, p.67.

Valenti,J. A. & Piskunov, N., 1996, A&AS, 118, p.595.